Defective spectrin integrity and neonatal thrombosis in the first mouse model for severe hereditary elliptocytosis

Nancy J. Wandersee, Amanda N. Roesch, Nancy R. Hamblen, Joost de Moes, Martin A. van der Valk, Roderick T. Bronson, J. Aura Gimm, Narla Mohandas, Peter Demant, and Jane E. Barker

Mutations affecting the conversion of spectrin dimers to tetramers result in hereditary elliptocytosis (HE), whereas a deficiency of human erythroid α- or β-spectrin results in hereditary spherocytosis (HS). All spontaneous mutant mice with cytoskeletal deficiencies of spectrin reported to date have HS. Here, the first spontaneous mouse mutant, *sph*^{Dem}/*sph*^{Dem}, with severe HE is described. The *sph*^{Dem} mutation is the insertion of an intracisternal A particle element in intron 10 of the erythroid α-spectrin gene. This causes exon skipping, the in-frame deletion of 46 amino acids from repeat 5 of α-spectrin and alters spectrin dimer/tetramer stability and osmotic fragility. The disease is more severe in *sph*^{Dem}/*sph*^{Dem} neonates than in α-spectrin–deficient mice with HS. Thrombosis and infarction are not, as in the HS mice, limited to adults but occur soon after birth. Genetic background differences that exist between HE and HS mice are suspect, along with red blood cell morphology differences, as modifiers of thrombosis timing. *sph*^{Dem}/*sph*^{Dem} mice provide a unique model for analyzing spectrin dimer-to-tetramer conversion and identifying factors that influence thrombosis. (Blood. 2001;97:543-550)

Introduction

The human diseases severe hereditary spherocytosis (HS) and severe hereditary elliptocytosis (HE) are defined by pronounced hemolysis, splenomegaly, and abnormally shaped red blood cells (RBCs).[1] The presence of elliptocytes and poikilocytes as well as spherocytes in peripheral blood smears differentiate HE from HS.[1] Mutations that cause HS and HE disrupt the cytoskeleton, a multiprotein complex responsible for the elasticity and durability of the circulating RBCs. Spectrin tetramers that comprise the cytoskeletal framework are composed of heterodimers of α and β subunits. These are tethered to the plasma membrane proteins AE1 (band 3) and glycophorin C through the ankyrin/protein 4.2 complex and through protein 4.1R and its associated actin filaments, respectively.[1] Mutations that decrease spectrin concentration or disrupt the association of spectrin with the plasma membrane result in HS.[2] Mutations that affect the conversion of spectrin dimers to spectrin tetramers result in HE.[2]

To date, all spontaneous mutations in α-spectrin (*Spna1*^{sph}, *Spna1*$^{sph\text{-}2BC}$, and *Spna1*$^{sph\text{-}J}$, hereafter, *sph*, *sph*^{2BC}, and *sph*^{J}) and β-spectrin (*Spnb1*^{ja}, hereafter, *ja*) that affect the RBC cytoskeleton in mice cause severe HS.[3] These mice have been instrumental in elucidating the genetic basis of the disease,[3] the distribution of red cell proteins,[4] and potential therapeutic measures.[5] Recently, we have shown that, as adults, the mutant mice develop thrombosis in many tissues.[5,6] Despite these thromboses, the mutant mice usually die of kidney failure accompanying progressive increases in hemosiderin.[5]

Until now, no spontaneous mutant mouse with HE has been described. This is unfortunate for 2 reasons. First, although the structural basis of spectrin dimerization and tetramerization has been elucidated in vitro, spectrin mutation sites in humans with HE suggest that lateral interactions in the heterodimer may affect tetramerization in vivo. A mouse model in which cell components have been genetically manipulated within cells with an otherwise identical genetic background could offer new insights into these interactions. Second, although the tissue distribution of erythroid spectrins is fairly well characterized, the pathologic differences between cells with an aberrant spectrin and those with a spectrin deficiency are not. In this report, we describe the first spontaneous mutation for HE in the mouse and compare its histopathology to mutants with HS.

Materials and methods

Animals

The *sph*^{Dem} mutation arose spontaneously on the CcS3/Dem recombinant congenic background. The CcS3/Dem colony is maintained through sib matings that generate wild type (+/+), heterozygous (*sph*^{Dem}/+), and homozygous (*sph*^{Dem}/*sph*^{Dem}) mice. The *ja*, *sph*, *sph*^{2BC}, and *sph*^{J} mutations are maintained as heterozygotes on both the WB/Re (WB) and C57BL/6J (B6) genetic backgrounds. Homozygous (*sph*/*sph*, *sph*^{2BC}/*sph*^{2BC}, and *sph*^{J}/*sph*^{J}) mutant mice are produced as WBB6F1 hybrids. Mice are housed and cared for according to Association for Assessment and Accreditation of Laboratory Animal Care (AAALAC) specifications.

From The Jackson Laboratory, Bar Harbor, ME; the Lawrence Berkeley National Laboratory, University of California-Berkeley, Berkeley, CA; the Division of Molecular Genetics, The Netherlands Cancer Institute, Amsterdam, The Netherlands; and Tufts University School of Veterinary Medicine, Boston, MA.

Submitted June 15, 2000; accepted September 19, 2000.

Supported by European Commission grants CHRXCT-930181 and BIO4-CT97-4850 to P.D., National Institutes of Health (NIH) grant R01 HL29305 to J.E.B., NIH grant R01 DK26263 to N.M., NIH grant NRSA F32 DK09482 to N.J.W., and NIH Core Grant CA34196 to The Jackson Laboratory.

Reprints: Jane E. Barker, The Jackson Laboratory, 600 Main St, Bar Harbor, ME 04609; e-mail: jeb@jax.org.

The publication costs of this article were defrayed in part by page charge payment. Therefore, and solely to indicate this fact, this article is hereby marked "advertisement" in accordance with 18 U.S.C. section 1734.

Complementation tests

Heterozygous *sph*^{Dem}/+ females were mated to male mice heterozygous for mutations in α-spectrin (*sph*, *sph*^{2BC}, *sph*^{J}) and β-spectrin (*ja*). Affected offspring were an indication that the mutation was an allele of the test gene.

Blood parameters and scanning electron microscopy

RBC count, hematocrit, hemoglobin, mean cell volume (MCV), and mean corpuscular hemoglobin concentration (MCHC) were obtained by standard methods.[7] Preparation of peripheral blood smears, reticulocyte enumeration, and scanning electron microscopy of RBCs were performed as previously described.[7] Mice were between 1.5 and 5 months of age at the time of hematologic assessment.

Osmotic gradient ektacytometry

Fresh blood samples were continuously mixed with a 4% polyvinylpyrrolidone solution of gradually increasing osmolality (from 60-600 mOsm). The deformability index was recorded as a function of osmolality at a constant applied shear stress of 170 dyne/cm^2 using an ektacytometer (Bayer Diagnostics, Tarrytown, NY).[8]

Sodium dodecyl sulfate-polyacrylamide gel electrophoresis (SDS-PAGE) and immunoblot analyses

RBC ghosts were prepared from packed red cells as previously described.[3] Equal amounts of ghost proteins were electrophoresed on 4% stacking/10% separating Laemmli SDS-PAGE gels. Duplicate gels were run; one was stained with Coomassie Brilliant Blue[9] and the other was transferred to Immobilon-P membranes (Millipore, Bedford, MA).[9,10] Immunostaining was performed using the Alkaline Phosphatase Conjugate Substrate Kit (Bio-Rad, Hercules, CA). Two different rabbit polyclonal antibodies to mouse purified erythroid spectrin were used: the first (used in Figure 2B) reacts similarly to α- and β-spectrin; the second (used in Figure 2E) reacts more strongly with α-spectrin than with β-spectrin.[11]

Spectrin extraction and PAGE separation of spectrin species

Spectrin extracts were prepared by incubation of RBC ghosts overnight at 0°C in low ionic strength buffer, followed by centrifugal separation of supernatant extracts and ghost residues.[12] Dimer and tetramer spectrin species were separated by electrophoresis on 2% to 4% gradient nondenaturing polyacrylamide gels and visualized by Coomassie Brilliant Blue staining.[13] Band intensities in both native and denaturing PAGE gels were quantified using a Molecular Dynamics (Sunnyvale, CA) Densitometer and Imagequant software.

Preparation of RNA

Reticulocytes from phenylhydrazine-treated normal[14] and mutant mice were isolated from heparinized blood collected by cardiac puncture. Spleens were obtained after transcardial perfusion of cold 1X phosphate-buffered saline (PBS; Gibco/BRL, Grand Island, NY). Total RNA was isolated using TRIZOL reagent (Gibco/BRL).

Northern analyses

Northern analyses were performed using the NorthernMax kit (Ambion, Austin, TX). Total RNA (5 μg) was separated by electrophoresis on 1% formaldehyde-based agarose gels in MOPS/sodium acetate/EDTA running buffer (Ambion) and transferred to BrightStar Plus membranes (Ambion). Equivalency of RNA loading was verified by UV shadowing.[15] Antisense RNA probe corresponding to nucleotides 7065 to 7322 of the murine erythroid α-spectrin complementary DNA (cDNA) sequence (GenBank accession no. AF093576) was produced by the Lig'n'Scribe kit (Ambion) and ^{32}P-labeled, using the StripEZ labeling kit and SP6 RNA polymerase (Ambion). Filters were hybridized at 65°C in NorthernMax hybridization buffer (Ambion). Final filter wash was at 65°C in 0.1X sodium chloride/sodium citrate (SSC), 0.1% SDS.

Reverse transcriptase-polymerase chain reaction (RT-PCR) and sequencing of normal and mutant α-spectrin alleles

RT-PCR was performed as previously described on total spleen RNA from CcS3/Dem-+/+ and CcS3/Dem-*sph*^{Dem}/*sph*^{Dem} mice.[16] Twelve overlapping RT-PCR fragments were generated to span the α-spectrin cDNA sequence. Fragments were sequenced by the dideoxynucleotide chain termination method,[17] using M13 forward and reverse primers and T7 DNA polymerase (TaqFS, ABI, Foster City, CA). Sequence data were analyzed using the Sequencher DNA analysis software package (ABI).

Genomic PCR and sequencing

Isolation and PCR of genomic spleen DNA from wild type (+/+), heterozygous (*sph*^{Dem}/+), and homozygous mutant (*sph*^{Dem}/*sph*^{Dem}) mice were performed as previously described.[18] PCR products were electrophoresed on 1% agarose gels. PCR products were sequenced and analyzed as described above. Long PCR of genomic DNA with primers 67 (5′-CCCTGGCTCTTCTAGTCT-3′) and 35 (5′-CTCTTGTCTGCTCATC-CAAC-3′) was carried out with the DyNAzyme EXT PCR system (Finnzyme).

Genomic DNA was isolated from tails of +/+ and *sph*^{Dem}/+ mice as previously described.[19] Tail DNA PCR was performed in 2 reactions, one using primers 67 and 35 (defined above), the other containing primers 67 and 69r (5′-TCCCTGATTGGCTGCAGCCCA-3′). The first reaction detects the wild type allele of *Spna1*; the second reaction detects the insertion in the *sph*^{Dem} allele. PCR products were electrophoresed on 2% SeaPlaque-GTG (FMC) agarose gels.

Histology

Heart, liver, kidney, and spleen were removed from euthanized adult mice after transcardial perfusion with 1X PBS followed by Bouin fixative. Neonates were fixed whole after euthanization. Embedded and sectioned tissues were stained with hematoxylin and eosin (H&E) or Gomori iron stain for nonhemoglobin iron.

Results

The new mutation, its origin, and allelism to α-spectrin mutations

The CcS3/Dem strain is one of 20 recombinant congenic strains produced between the BALB/cHeA and STS/A inbred strains.[20-22] In 1991, a recessive mutation arose spontaneously on the CcS3/Dem background in the colonies of Dr P. Demant at The Netherlands Cancer Institute. Initial observations identified normocytes and stipple cells in neonatal blood. Mutant neonates were jaundiced and had liver degeneration. Older mutants exhibited hyperplastic erythropoiesis in spleen and bone marrow, splenomegaly, and liver and kidney degeneration. The mutant mice were imported to The Jackson Laboratory by Dr Barker in 1996.

Initial observations suggested the mutant mice had hemolytic anemia. Matings between heterozygotes for the new mutation and heterozygotes for the *sph*, *sph*^{2BC}, and *sph*^{J} mutations in α-spectrin, but not the *ja* mutation in β-spectrin, produced mutant offspring (Table 1). The new mutation in the erythroid α-spectrin gene, *Spna1*, was designated *sph*^{Dem} to reflect its allelism to existing α-spectrin mutations.

Hematologic analysis of *sph*^{Dem}/*sph*^{Dem} mice is consistent with severe HE

sph^{Dem}/*sph*^{Dem} mice suffer from severe anemia characterized by RBC counts, hematocrits, and hemoglobins that are 48%, 57%, and 38% of normal, respectively (Table 2). MCV is increased and MCHC is decreased in the mutants, most likely reflecting the

Table 1. The new mutation (*nm*) is allelic to *sph*, *sph*^{2BC}, and *sph*^{J} mutations

Complementation cross (×)*	No. mutants†/No. in litter
nm/+ × *sph*/+	2/8
nm/+ × *sph*^{2BC}/+	2/6
nm/+ × *sph*^{J}/+	1/6
nm/+ × *ja*/+	0/7
nm/+ × *ja*/+	0/5

*Genotype of female indicated first, genotype of male second.
†Mutants are identified by their neonatal jaundice.

marked reticulocytosis (50%). Blood parameters in heterozygous (*sph*^{Dem}/+) mice mirrored those seen in +/+ mice (data not shown).

Peripheral blood smears reveal the presence of elliptocytic as well as spherocytic and occasional poikilocytic RBCs in *sph*^{Dem}/*sph*^{Dem} mice (Figure 1A). Scanning electron microscopy confirms the variability in RBC shapes (Figure 1B). The variety of RBC shapes observed in *sph*^{Dem}/*sph*^{Dem} mice are in stark contrast to the strictly spherocytic RBCs observed in all other mice described to date with cytoskeletal defects.[3,7] The observations in *sph*^{Dem}/*sph*^{Dem} mice are consistent with observations made in peripheral blood smears from humans with severe HE. Blood smears and scanning electron microscopy of RBCs from heterozygous mice revealed no abnormalities (data not shown).

Osmotic deformability profiles of blood samples from wild type (+/+), heterozygous (+/−) and homozygous *sph*^{Dem}/*sph*^{Dem} (−/−) mice are shown in Figure 1C. The maximum value of the deformability index attained at physiologically relevant osmolality (DImax) is quantitatively related to the mean surface area of the cells.[8] The osmolality at which the deformability index reaches a minimum in the hypotonic region of the gradient (Omin) is a measure of the osmotic fragility of the cells.[8] RBCs from heterozygotes do not have significantly different osmotic deformability profiles than wild type RBCs. In contrast, RBCs from *sph*^{Dem}/*sph*^{Dem} mice exhibit a profound decrease in surface area (decreased DImax) and a marked increase in osmotic fragility (increased Omin). The decrease in surface area is consistent with the marked fragmentation of the *sph*^{Dem}/*sph*^{Dem} RBCs and is slightly less than the decrease in surface area observed in *sph/sph* RBCs (relative decrease in DImax compared to wild type of 54% versus 70% for *sph/sph*).[16]

Hereditary pyropoikilocytosis (HPP) is distinguished from severe HE in humans by increased thermal sensitivity of HPP RBCs relative to HE (or HS) RBCs.[23] Accordingly, we attempted to use established protocols to determine whether *sph*^{Dem}/*sph*^{Dem} RBCs exhibited increased thermal sensitivity. Unfortunately, mouse RBCs do not react in these tests in the same manner as human RBCs, and we were unable to measure the thermal sensitivity of *sph*^{Dem}/*sph*^{Dem} versus +/+ RBCs (data not shown).

sph^{Dem}/*sph*^{Dem} mice are deficient in erythroid spectrin

Coomassie Blue-stained SDS-PAGE gels of RBC ghosts show an extreme deficiency of spectrin and ankyrin in *sph*^{Dem}/*sph*^{Dem} mice: α-spectrin:band 3 is 1.3% of normal, β-spectrin:band 3 is 4.4% of normal, and ankyrin:band 3 is 10% of normal (Figure 2A and Table 3). Immunoblot analyses (Figure 2B) of RBC ghosts with an antibody that reacts similarly to α- and β-spectrin confirm that *sph*^{Dem}/*sph*^{Dem} mice are deficient in both α- and β-spectrin. An aberrant 65-kd immunoreactive protein is seen in *sph*^{Dem}/*sph*^{Dem} ghosts that is not observed in other mutant mice. Immunoblot analyses with an antibody that detects α-spectrin more efficiently than β-spectrin suggest that this aberrant protein is a fragment of α-spectrin (see below).

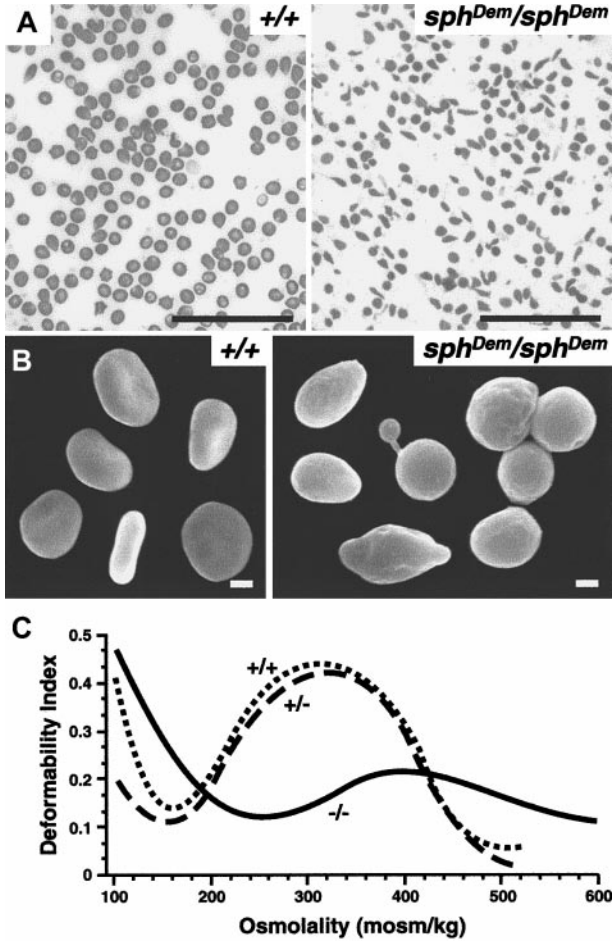

Figure 1. *sph*^{Dem}/*sph*^{Dem} mice have severe HE. (A) Wright-stained peripheral blood smears from +/+ (left panel) and *sph*^{Dem}/*sph*^{Dem} (right panel) mice. Note the presence of spherocytic, elliptocytic, poikilocytic, and fragmented RBCs in the mutant mice. Bar, 5 μm. (B) Scanning electron microscopy of RBCs from +/+ (left panel) and *sph*^{Dem}/*sph*^{Dem} (right panel). Note the abnormally shaped RBCs in the mutant. Bar, 1 μm. (C) Osmotic deformability profiles of RBCs from wild type (+/+), heterozygous (*sph*^{Dem}/+), and homozygous (*sph*^{Dem}/*sph*^{Dem}) mice.

Native and denaturing PAGE suggests defective dimer/tetramer stability in *sph*^{Dem}/*sph*^{Dem} mice

Humans with HE show an increase in the spectrin dimer-to-tetramer ratio.[1] Spectrin dimer-to-tetramer ratios were compared in

Table 2. Blood parameters in *sph*^{Dem}/*sph*^{Dem} and normal mice

Genotype (No. of mice)	RBC count (×10^{12}/L)	Hematocrit (%)	Hemoglobin (g/dL)	MCV (μm^3)	MCHC (g/dL)	Reticulocyte (%)
+/+ (7)	11.24 ± 0.43	52.9 ± 1.9	14.4 ± 0.6	47.3 ± 1.9	27.1 ± 0.4	2
sph^{Dem}/*sph*^{Dem} (15)	5.36 ± 0.27	30.1 ± 1.3	5.5 ± 0.3	56.9 ± 2.0	18.4 ± 0.5	50

All values except reticulocyte percentages are mean ± SEM; all mutant values are significantly different ($P \leq .005$). RBC = red blood cell; MCV = mean cell volume; MCHC = mean corpuscular hemoglobin concentration.

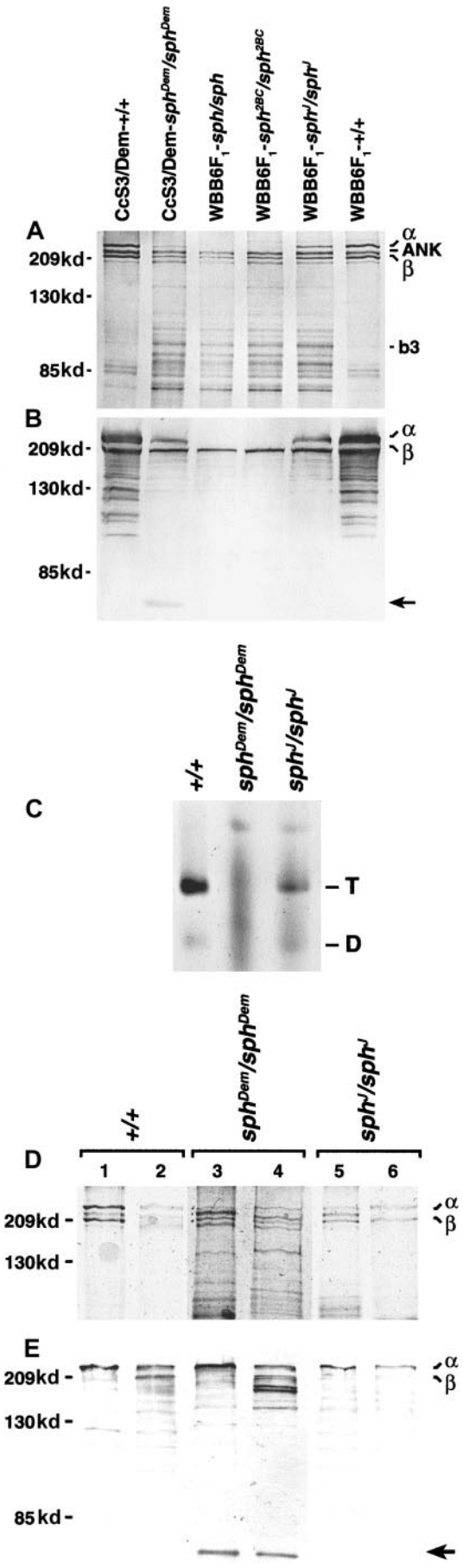

extracts from +/+, *sph*^{Dem}/*sph*^{Dem}, *sph/sph*, *sph*^{2BC}/*sph*^{2BC}, and *sph*^{J}/*sph*^{J} RBC ghosts. These extracts were analyzed by native PAGE (Figure 2C). Spectrin extracts from the negative controls, *sph/sph* and *sph*^{2BC}/*sph*^{2BC}, do not have detectable α-spectrin monomer (Figure 2A,B) and do not contain either spectrin dimers or tetramers (data not shown). The dimer-to-tetramer ratio is similar in +/+ and *sph*^{J}/*sph*^{J} extracts (0.14:1 and 0.1:1, respectively; Figure 2C legend). In contrast, distinct dimer and tetramer bands are not resolved from *sph*^{Dem}/*sph*^{Dem} spectrin extracts (Figure 2C, lane 2). SDS-PAGE analyses (Figure 2D) reveal no increase in protein bands in spectrin extracts (lanes 2, 4, 6) as compared to RBC ghosts (lanes 1, 3, 5). The amount of apparently full-length α- and β-spectrin monomer in *sph*^{Dem}/*sph*^{Dem} spectrin extract is similar to the monomer amounts in *sph*^{J}/*sph*^{J} spectrin extracts, suggesting that sufficient monomers are present to generate detectable dimers and tetramers. Immunoblot analyses with an antibody that reacts more strongly to α- than β-spectrin (Figure 2E) confirm the presence of immunoreactive fragments in +/+, *sph*^{Dem}/*sph*^{Dem}, and *sph*^{J}/*sph*^{J} spectrin extracts. The segregation of presumed proteolytic fragments immediately below β-spectrin in *sph*^{Dem}/*sph*^{Dem} spectrin extracts but not in *sph*^{J}/*sph*^{J} spectrin extracts raises the possibility that these fragments may interfere with proper association of full-length monomers. The strong labeling of the 65-kd protein in both *sph*^{Dem}/*sph*^{Dem} ghosts and spectrin extracts with this antibody suggests that it is a fragment of α-spectrin that segregates with the spectrin fraction in extracts.

Identification of the molecular defect in the α-spectrin gene in *sph*^{Dem}/*sph*^{Dem} mice

The erythroid α-spectrin transcript levels in *sph*^{Dem}/*sph*^{Dem} spleen and reticulocytes are decreased when compared to transcript levels in +/+ tissues (Figure 3A). The decrease in mutant α-spectrin transcript is more pronounced in reticulocytes than spleen. This suggests that the mutant α-spectrin transcript is unstable and is degraded as erythroid precursors mature. Transcripts encoding the 65-kd protein seen on immunoblots could not be clearly resolved.

The presence of α-spectrin mRNA in *sph*^{Dem}/*sph*^{Dem} spleen allowed us to utilize RT-PCR techniques to identify the *sph*^{Dem} mutation. Comparison of cDNA sequence from +/+ and *sph*^{Dem}/*sph*^{Dem} mice indicated that exon 11 was absent in *sph*^{Dem}/*sph*^{Dem} α-spectrin messenger RNA (mRNA). This 138 nucleotide (nt) deletion results in the in-frame deletion of 46 amino acids (aa) from

Figure 2. *sph*^{Dem}/*sph*^{Dem} mice have defective dimer/tetramer complexes. (A) SDS-PAGE of RBC ghost proteins from +/+ (lanes 1, 6) and mutant (lanes 2, 3, 4, 5) mice. Strain background and genotype of mice are indicated above each lane. Size markers indicated on left; relative positions of α-spectrin (α), ankyrin (ANK), β-spectrin (β), and band 3 (b3) indicated on right. Ratios of α, ANK, and β to b3 are listed in Table 3. (B) Immunoblot of RBC ghost proteins from +/+ (lanes 1, 6) and mutant (lanes 2, 3, 4, 5) mice. Strain background and genotype of mice are indicated above each lane. Primary antibody detects α- and β-spectrin equally. Size markers indicated on left; relative positions of α- and β-spectrin indicated on right. Arrow on right marks position of the 65-kd immunoreactive protein in *sph*^{Dem}/*sph*^{Dem} mice (lane 2). (C) Representative native PAGE of 0°C low ionic strength spectrin extracts from RBC ghosts of +/+ (lane 1) and mutant (lanes 2, 3) mice stained with Coomassie Blue. Genotype of mice is indicated above each lane. Positions of spectrin dimers [D] and tetramers [T] are indicated on right. Densitometric values (in pixels): +/+[D] = 60; +/+[T] = 425; +/+[D]:[T] ratio = 0.14:1; *sph*^{J}/*sph*^{J}[D] = 11; *sph*^{J}/*sph*^{J}[T] = 109; *sph*^{J}/*sph*^{J}[D]:[T] ratio = 0.10:1. (D) SDS-PAGE of RBC ghost (lanes 1, 3, 5) and spectrin extract (lanes 2, 4, 6) proteins from +/+ (lanes 1, 2) and mutant (lanes 3-6) mice. Genotype of mice is indicated above each pair of lanes. Size markers indicated on left; positions of α- and β-spectrin indicated on right. (E) Immunoblot of RBC ghost (lanes 1, 3, 5) and spectrin extract (lanes 2, 4, 6) proteins from +/+ (lanes 1, 2) and mutant (lanes 3-6) mice. Genotype of mice is indicated above each pair of lanes. Primary antibody detects α-spectrin more efficiently than β-spectrin. Size markers indicated on left; positions of α- and β-spectrin indicated on right. Arrow on right marks 65-kd immunoreactive protein in *sph*^{Dem}/*sph*^{Dem} mice (lanes 3, 4).

Table 3. Relative amounts of α-spectrin, ankyrin, and β-spectrin in normal and mutant mice

Genotype	α:b3	ANK:b3	β:b3
CcS3/Dem-+/+	27.7	13.0	26.6
CcS3/Dem-*sph^{Dem}/sph^{Dem}*	0.4	1.3	1.2
WBB6F1-*sph/sph*	0	1.3	1.2
WBB6F1-*sph^{2BC}/sph^{2BC}*	0	1.6	1.6
WBB6F1-*sph^{J}/sph^{J}*	1.7	2.0	2.8
WBB6F1-+/+	22.0	7.9	20.0

Amounts based on densitometry of α-spectrin (α), β-spectrin (β), ankyrin (ANK), and band 3 (b3) in the sodium dodecyl sulfate-polyacrylamide gel electrophoresis gel shown in Figure 2A.

repeat 5 of the α-spectrin protein (Figure 3B,C). No other anomalies were found in the mutant α-spectrin cDNA sequence.

Amplification of genomic spleen DNA using exon 11-specific primers showed that exon 11 is present in the genomic DNA of *sph^{Dem}/sph^{Dem}* mice (data not shown). This suggested a mutation within exon 11 or flanking introns resulting in aberrant splicing and the skipping of exon 11 in the mature mRNA. Sequencing of exon 11 and intron 11 from genomic DNA revealed no discrepancies between normal and mutant sequences (data not shown). Sequencing of all but the most 3′ portion of intron 10 did not identify sequence abnormalities in *sph^{Dem}/sph^{Dem}* genomic DNA (data not shown). Attempts to amplify the 3′ end of intron 10 from mutant DNA failed, suggesting a large insertion was present.

Southern blot analyses indicated that the insertion in the *sph^{Dem}* allele was between 3 and 6 kilobases (kb) in length (data not shown). Standard genomic PCR using primers 67 and 35 (Figure 4A), only 350 base pairs (bp) apart in the normal allele, failed to yield a product from *sph^{Dem}/sph^{Dem}* DNA (data not shown). Long-range genomic PCR produced a product of approximately 5.75 kb from heterozygous (*sph^{Dem}*/+) and mutant (*sph^{Dem}/sph^{Dem}*) DNA, and the expected 350 bp product from wild type (+/+) and heterozygous (*sph^{Dem}*/+) DNA (Figure 4B).

The size of the insert is similar to that reported for ETn transposons and deleted type I intracisternal A particle (IAP) elements.[24-28] Genomic PCR with primers 67 or 35 paired with primers specific for the long terminal repeat (LTR) of ETn transposons (kindly provided by V. Letts, The Jackson Laboratory) failed to yield products (data not shown). Amplification using primers 67 or 35 paired with primers specific for IAP LTRs (69 and 69r, Figure 4A; kindly provided by B. Gwynn, The Jackson Laboratory) generated products from *sph^{Dem}/sph^{Dem}* and *sph^{Dem}*/+ DNA, but not from +/+ DNA (data not shown). To confirm that the insertion of the IAP element is the *sph^{Dem}* mutation, genomic PCR of tail DNA from known +/+ and *sph^{Dem}*/+ mice was performed. PCR with primers designed to identify the normal α-spectrin allele yields a product in both +/+ and *sph^{Dem}*/+ mice (Figure 4C, lanes 35). Amplification with primers designed to identify the α-spectrin IAP insertion is successful only in *sph^{Dem}*/+ mice (Figure 4C, lanes 69r). These data confirm that the insertion of the IAP element segregates with the *sph^{Dem}* mutation.

Additional sequencing identified the exact location of the insertion of IAP element within the α-spectrin gene. The IAP element is at the junction between intron 10 and exon 11; a target site duplication of the first 6 bp of exon 11 occurs at the 5′ junction of the IAP insertion (Figure 4A). In Figure 4D, portions of the LTR sequence obtained for the IAP element in the *sph^{Dem}* α-spectrin allele (middle line) are compared with consensus LTR sequences of IAP elements in the T (top line) and LS (bottom line) subclasses. The LTR sequences of the IAP element inserted into *sph^{Dem}* α-spectrin allele are identical to those of the T subclass of IAP elements.

Pathology of neonatal *sph^{Dem}/sph^{Dem}* mice differs from that in *sph/sph* mice

A high percentage of *sph^{Dem}/sph^{Dem}* mice do not survive the neonatal period; only 32% of *sph^{Dem}/sph^{Dem}* neonates survive to weaning at 4 weeks of age, compared with 70% of *sph/sph* neonates (Table 4). Unlike *sph/sph* and +/+ neonates, cardiac or liver thrombi are present in approximately 69% of *sph^{Dem}/sph^{Dem}* neonates, whereas liver infarctions are observed in 88% of *sph^{Dem}/sph^{Dem}* neonates (Table 4, Figure 5A-D, and data not shown).

Pathology of adult *sph^{Dem}/sph^{Dem}* mice

The average life span of *sph^{Dem}/sph^{Dem}* mice that survive to weaning is 2.5 months, compared to 6.7 months for *sph/sph* mice (Table 4) and approximately 24 months for normal mice. Spleen-to-body weight, heart-to-body weight, and liver-to-body weight ratios are all increased in *sph^{Dem}/sph^{Dem}* mice, and the spleens are highly erythroid, comparable to observations made in *sph/sph* mice.[5,6] Similar to *sph/sph* mice, a high percentage of adult *sph^{Dem}/sph^{Dem}*

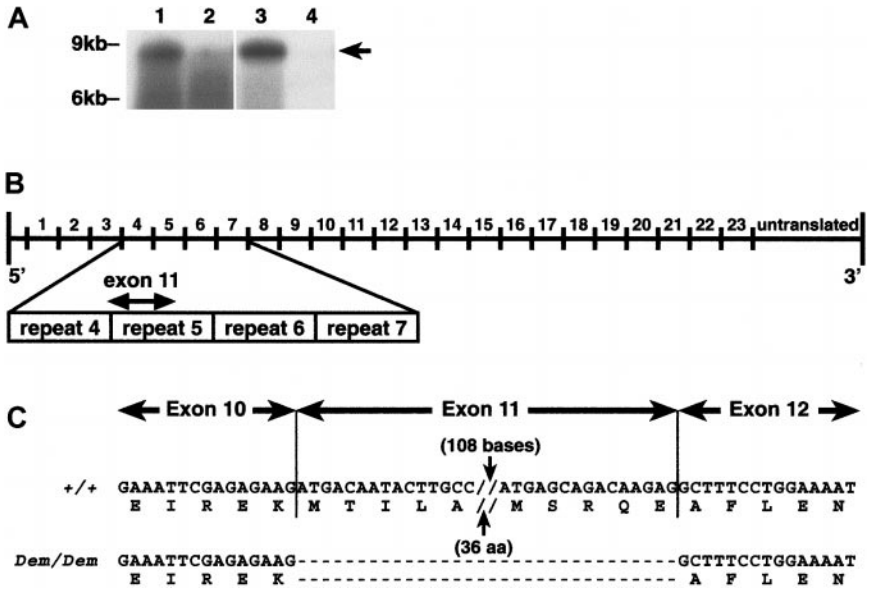

Figure 3. Analysis of *sph^{Dem}/sph^{Dem}* cDNA sequence. (A) Northern blots of total RNA from spleen (lanes 1, 2) and reticulocytes (lanes 3, 4) of +/+ (lanes 1, 3) and *sph^{Dem}/sph^{Dem}* (lanes 2, 4) mice. UV shadowing was used to check RNA loading. Size markers are indicated on the left. Arrow on right identifies the +/+ 8-kb transcript. (B) Schematic representation of the *Spna1* cDNA with numbers above the line corresponding to the repeats of 106 aa that comprise the α-spectrin protein. Shown below the cDNA schematic is an enlargement of repeats 4 through 7 of α-spectrin, with the location of exon 11 identified. (C) α-Spectrin cDNA sequence obtained from spleen RNA of wild type (+/+) and *sph^{Dem}/sph^{Dem}* (*Dem/Dem*) mice. Shown directly below each cDNA sequence is the corresponding protein sequence. Note the lack of exon 11 sequence in the cDNA from *sph^{Dem}/sph^{Dem}* mice and that this deletion does not alter the translational reading frame.

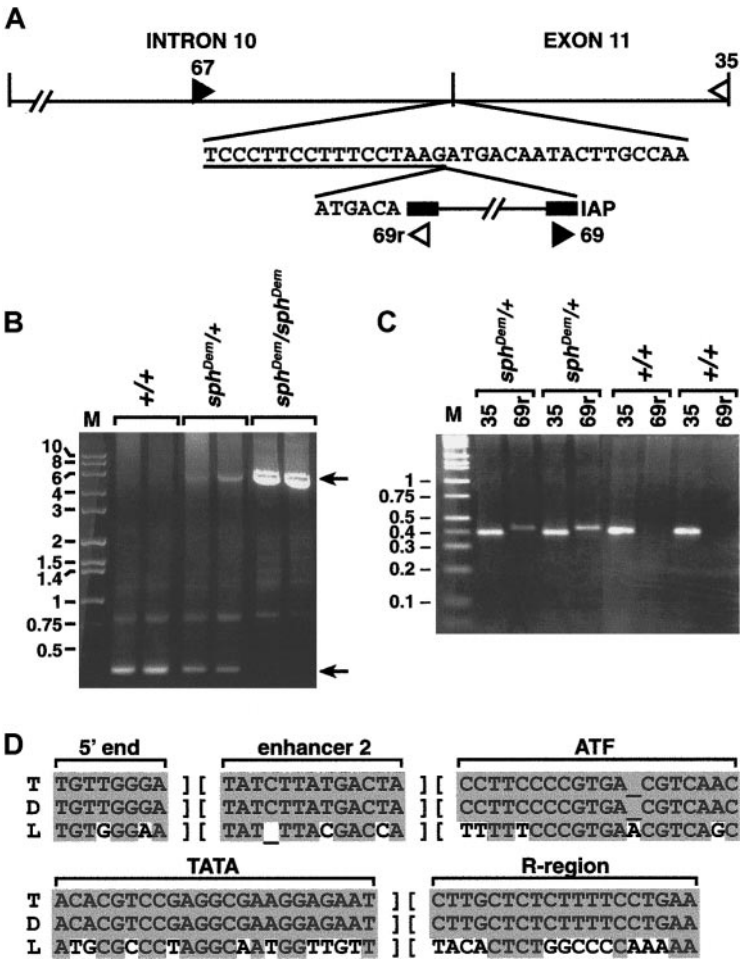

Figure 4. Analysis of *sph*^{Dem}/*sph*^{Dem} genomic DNA. (A) Top line, schematic of intron 10 and exon 11 of the *Spna1* gene. Vertical lines denote exon/intron boundaries. Second line, normal sequence at the intron 10/exon 11 boundary; intron sequence is underlined. The IAP element present in the *sph*^{Dem} allele is shown on the third line, flanked by its LTR sequences (black boxes). The 6 bases preceding the IAP element on the third line represent exon 11 sequence duplicated by insertion of the element. Double hatch (//) marks denote sequence not represented in the figure. Filled and open triangles show the location of forward and reverse PCR primers, respectively. Sequence of PCR primers 67, 35, and 69r is found in the "Materials and methods" section; primer 69 is the complement of primer 69r. (B) Long PCR of genomic DNA from +/+ (lanes 2, 3), *sph*^{Dem}/+ (lanes 4, 5), and *sph*^{Dem}/*sph*^{Dem} (lanes 6, 7) mice with primers 67 and 35. M, marker lane, sizes of markers in kb are indicated on left. Top arrow on right identifies the 5.75-kb band resulting from amplification of the insert-containing *sph*^{Dem} allele of *Spna1*. Bottom arrow on right identifies the 0.35-kb band resulting from amplification of the normal allele of *Spna1*. (C) Genomic PCR of tail DNA from 2 different +/+ and *sph*^{Dem}/+ mice. Lane M is marker; sizes in kb are shown on left. Lanes '35': PCR products from a reaction containing primers 67 and35 that will amplify the wild type allele of *Spna1*. Lanes '69r': PCR products from a reaction containing primers (67 and 69r) designed to identify the IAP insertion in the *sph*^{Dem} allele. Genotype of mice is noted above each bracketed pair of reactions. (D) The *sph*^{Dem} IAP is in the T subclass. Sequences of LTR elements derived from LS-type ('L', bottom line)[24] and T-type ('T', top line)[25,26] IAP elements compared to that of the IAP element inserted in intron 10 of the *sph*^{Dem} allele of *Spna1* ('D', middle line). The regions of sequence shown are used to classify IAP elements.[24] Shaded bases represent sequence identity; nonshaded bases represent sequence divergence.

mice have cardiac thrombi. Unlike *sph/sph* mice, cardiac thrombi are observed in *sph*^{Dem}/*sph*^{Dem} mice younger than 6 weeks of age (data not shown).

The kidneys of *sph*^{Dem}/*sph*^{Dem} mice show glomerulonephritis and accumulation of hemosiderin-laden casts in the renal tubules. The concentration of renal hemosiderin is less in *sph*^{Dem}/*sph*^{Dem} mice (Figure 5F) than in *sph/sph* mice (Figure 5E). Similarly, extramedullary hematopoiesis in the liver of *sph*^{Dem}/*sph*^{Dem} mice (arrowheads, Figure 5I,K) is less than that observed in *sph/sph* mice (arrowheads, Figure 5G). *sph*^{Dem}/*sph*^{Dem} mice frequently have calcified lesions in the liver (arrows, Figure 5I) that are indicative of infarctions that likely occurred in the neonatal period. Such calcified lesions are not seen in the livers of *sph/sph* mice (Figure 5G). Unlike *sph/sph* mice, which show pervasive hemosiderin deposition in hepatocytes (Figure 5H), *sph*^{Dem}/*sph*^{Dem} mice show little or no hemosiderin (Figure 5L), except in regions of liver immediately surrounding calcified lesions (Figure 5J). The histopathology noted in both *sph/sph* and *sph*^{Dem}/*sph*^{Dem} mice is not seen in +/+ mice.[5,6]

Table 4. Life span and thrombotic prevalence in *sph*^{Dem}/*sph*^{Dem} versus *sph/sph* mice

Genotype	Neonates surviving to wean (%)	Neonates with thrombi* (%)	Average life span of weaned mice (m)	Adults† with cardiac thrombi (%)
sph^{Dem}/*sph*^{Dem}	32 (n = 120)	69 (n = 16)	2.5 (n = 65)	95 (n = 21)
sph/sph	70 (n = 130)	0 (n = 23)	6.7 (n = 60)	100 (n = 45)

n = total number of animals studied for each measurement.
*Cardiac or liver thrombi.
†Adult = 10 weeks of age or older.

Discussion

In the present study, we describe *sph*^{Dem}/*sph*^{Dem} mice with a mutation in erythroid α-spectrin that represents the first mouse model for severe HE in humans. The lack of HE in mice with cytoskeletal deficiencies until this point has prompted many to presume that physiologic and/or physical differences in mouse RBCs prevent the assumption of an elliptocytic or poikilocytic shape. It is possible that mice with mild or asymptomatic HE would remain undetected unless a blood smear was performed. Reanalysis in light of the current discovery and the molecular definition of preexisting mutations causing HS provide another explanation for the lack of HE in previous mouse mutants. HS results from spectrin deficiency; HE results from disruption of dimer-to-tetramer conversion through mutations in protein 4.1R, β-spectrin, or α-spectrin.[2] Mouse protein 4.1R-deficient RBCs, in contrast to human protein 4.1R-deficient RBCs, are also deficient in spectrin, which may explain their spherocytic rather than elliptocytic appearance.[29] β-Spectrin-deficient *ja/ja* mice have a nonsense mutation in β-spectrin repeat 9, causing complete deficiency of both α- and β-spectrin.[4]

Three α-spectrin mouse mutants, *sph/sph*, *sph*^{2BC}/*sph*^{2BC}, and *sph*^{J}/*sph*^{J}, have HS. The *sph*^{2BC} and *sph*^{J} mutations are in the 3′ end of α-spectrin, distant from the self-association site,[30] and do not affect tetramerization (Figure 2). In fact, *sph*^{J} α-spectrin tetramerizes, but the α-spectrin is not stably bound to the membrane,

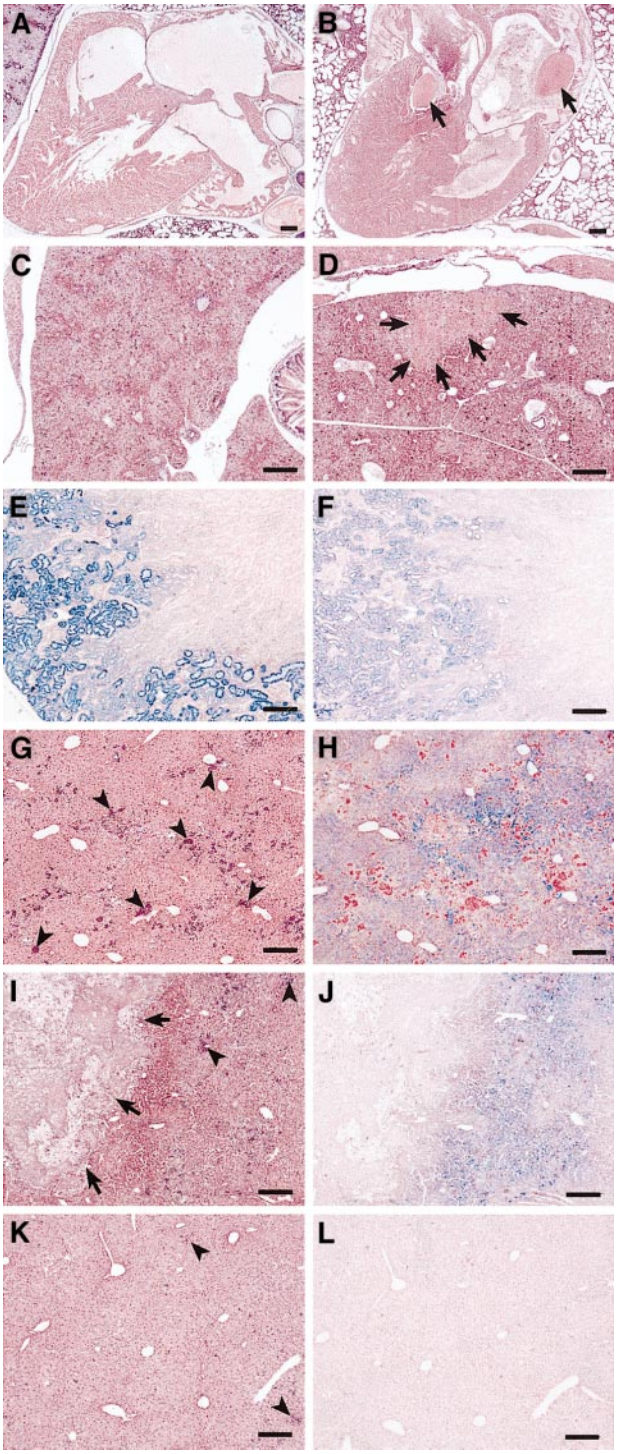

Figure 5. Histopathology of neonatal and adult *sph*^{Dem}/*sph*^{Dem} mice. Histological sections of heart, liver, and kidney from *sph/sph* and *sph*^{Dem}/*sph*^{Dem} mice. Bars = 20 μm. (A, C, E, G, H): *sph/sph*. (B, D, F, I, J, K, L): *sph*^{Dem}/*sph*^{Dem}. (A,B): Heart sections of neonates stained with H&E. Note the presence of thrombi (indicated by arrows) in the valve and atrium of (B). (C,D): Liver sections from neonates stained with H&E. Note the presence of an infarcted region (identified by arrows) in (D). (E,F): Kidney sections from adult mice, stained with Gomori iron stain, which stains nonhemoglobin iron blue. (G,I,K): Liver sections from adult mice stained with H&E. Clusters of extramedullary hematopoiesis (arrowheads) stain purple. Arrows in (I) identify a large calcified lesion indicative of earlier infarction. (H,J,L): Identical regions of liver as shown in (G,I,K), stained with Gomori iron stain.

resulting in spectrin deficiency.[3] The *sph* mutation is a single-base deletion in repeat 5 of α-spectrin, resulting in a complete absence of α-spectrin.[16] The *sph*^{Dem} mutation, although near the *sph* mutation, produces different effects. The IAP insertion leads to the in-frame deletion of 46 amino acids from repeat 5 of α-spectrin; the apparently full-length product observed in immunoblot analyses is most likely the deleted protein. The location of the *sph*^{Dem} mutation is similar to the location of several mutations associated with human HE that produce in-frame deletions in α-spectrin.[2] Like *sph*^{Dem}, one of these human HE mutations, spectrin Dayton, is also the result of the insertion of a mobile DNA element.[31] The insertion of mobile DNA elements does not always lead to a mutant phenotype. In *sph*^{Dem} and spectrin Dayton, the location of the mobile element likely disrupts normal scanning and splicing, leading in both cases to exon skipping and protein disruption.

The RBC morphology seen in *sph*^{Dem}/*sph*^{Dem} mice is consistent with that seen in human severe HE.[2] Several human α-spectrin mutations associated with severe HE, notably α^{Alexandria}, α$^{St\ Claude}$, α^{Oran}, and α^{Barcelona}, occur at equivalent or greater distances from the tetramerization site as *sph*^{Dem}.[32-35] The severe effect of mutations distant from the minimal tetramerization site suggests that structural flexibility in vivo affects spectrin dimer-to-tetramer conversion. The *sph*^{Dem} mutation provides an easily accessible model system in which to examine structural integrity and dimer-to- tetramer conversion in vivo. Although the *sph*^{Dem} mutation is 3′ to the previously described minimal α-spectrin tetramerization site,[36,37] the deletion in the *sph*^{Dem} protein nevertheless destabilizes both dimer and tetramer structure, suggesting that the deleted amino acids are central to tetramerization. Additional immunoblot analyses with region-specific antibodies as well as direct sequencing of the aberrant 65-kd protein seen on Western blots will provide information on the nature and identity of this fragment and possible contributions to the mutant phenotype.

The difference in pathology between *sph*^{Dem}/*sph*^{Dem} and *sph/sph* mice may be related to disparate pathologic effects of elliptocytic versus spherocytic RBCs, respectively. Alternatively, genetic differences between the strain background of the *sph*^{Dem} and *sph* mutations (CcS3/Dem versus WBB6F1, respectively) may affect the pathology of the mutant mice. The latter possibility is being addressed by transferring the *sph*^{Dem} mutation onto the WBB6F1 background and assessing any changes in the pathology of *sph*^{Dem}/*sph*^{Dem} neonates or adults. The most intriguing difference in the pathology of *sph*^{Dem}/*sph*^{Dem} mice is the much earlier initiation of thrombosis as compared to *sph/sph* mice (neonatal versus 6 weeks of age, respectively). Neonatal thrombosis has also been noted in one line of band 3 knockout mice maintained on yet another mixed genetic background.[38] Thrombotic events affect a small number of patients with HS but a much larger percentage of patients with β-thalassemia or sickle cell disease.[39-43] Analyses of the pathophysiologic and/or genetic factors responsible for the earlier initiation of thrombosis in *sph*^{Dem}/*sph*^{Dem} mice will increase our understanding of thrombogenesis in the context of hemolytic anemia and will provide a means to identify those patients at increased risk for developing thrombotic complications.

Acknowledgments

The authors thank Luanne Peters, David Serreze, and Babette Gwynn for critical review of the manuscript. We thank Verity Letts and Babette Gwynn for sharing ETn-specific and IAP-specific primers, and Katherine John for discussions on dimer/tetramer analyses. We greatly appreciate the technical assistance of Lesley Bechtold in Biological Imaging, Amy Lambert and Andrea Ried in Microchemistry Services, and Jennifer Smith in Graphics Services at The Jackson Laboratory.

References

1. Lux SE, Palek J. Disorders of the red cell membrane. In: Handin RI, Lux SE, Stossel TP, eds. Blood: Principles and Practice of Hematology. Philadelphia, PA: Lippincott; 1995:1733-1765.
2. Tse WT, Lux SE. Red blood cell membrane disorders. Br J Haematol. 1999;104:2-13.
3. Barker JE, Bodine DM, Birkenmeier CS. Synthesis of spectrin and its assembly into the red blood cell cytoskeleton of normal and mutant mice. In: Bennett V, Lux SE, Cohen CM, Palek J, eds. Membrane Skeletons and Cytoskeletal-Membrane Associations. New York, NY: Liss; 1986: 313-324.
4. Bloom ML, Kaysser TM, Birkenmeier CS, Barker JE. The murine mutation jaundiced is caused by replacement of an arginine with a stop codon in the mRNA encoding the ninth repeat of β-spectrin. Proc Natl Acad Sci U S A. 1994;91:10099-10103.
5. Kaysser TM, Wandersee NJ, Bronson RT, Barker JE. Thrombosis and secondary hemochromatosis play major roles in the pathogenesis of jaundiced and spherocytic mice, murine models for hereditary spherocytosis. Blood. 1997;90:4610-4619.
6. Wandersee NJ, Lee JC, Kaysser TM, Bronson RT, Barker JE. Hematopoietic cells from α-spectrin deficient mice are sufficient to induce thrombotic events in hematopoietically ablated recipients. Blood. 1998;92:4856-4863.
7. Peters LL, Birkenmeier CS, Barker JE. Fetal compensation of the hemolytic anemia in mice homozygous for the normoblastosis (*nb*) mutation. Blood. 1992;80:2122-2127.
8. Clark MR, Mohandas N, Shohet SB. Osmotic gradient ektacytometry: comprehensive characterization of red cell volume and surface maintenance. Blood. 1983;61:899-910.
9. Laemmli UK. Cleavage of structural proteins during the assembly of the head of bacteriophage T4. Nature. 1970;227:680-685.
10. White RA, Birkenmeier CS, Lux SE, Barker JE. Ankyrin and the hemolytic anemia mutation, *nb*, map to mouse chromosome 8: presence of the *nb* allele is associated with a truncated erythrocyte ankyrin. Proc Natl Acad Sci U S A. 1990;87:3117-3121.
11. Bodine DM IV, Birkenmeier CS, Barker JE. Spectrin deficient inherited hemolytic anemias in the mouse: characterization by spectrin synthesis and mRNA activity in reticulocytes. Cell. 1984;37: 721-729.
12. Liu S-C, Windisch P, Kim S, Palek J. Oligomeric states of spectrin in normal erythrocyte membranes: biochemical and electron microscopic studies. Cell. 1984;37:587-594.
13. Morrow JS, Haigh WB. Erythrocyte membrane proteins: detection of spectrin oligomers by gel electrophoresis. Methods Enzymol. 1983;26: 298-304.
14. Chui DHK, Patterson M, Bayley ST. Unequal α and β globin mRNA in reticulocytes of normal and mutant (*f/f*) fetal mice. Br J Haematol. 1980;44: 431-439.
15. Thurston SJ, Saffer JD. Ultraviolet shadowing nucleic acids on nylon membranes. Anal Biochem. 1989;178:41-42
16. Wandersee NJ, Birkenmeier CS, Gifford EJ, Mohandas N, Barker JE. Murine hereditary spherocytosis, *sph/sph*, is caused by a mutation in the erythroid α-spectrin gene. The Hematology Journal. 2000;1:235-242.
17. Sanger F, Nicklen S, Coulson AR. DNA sequencing with chain-terminating inhibitors. Proc Natl Acad Sci U S A. 1977;74:5463-5467.
18. Chang YA, Mold DE, Brilliant MH, Huang RC. The mouse intracisternal-A particle-promoted placental gene retrotransposition is mouse-strain-specific. Proc Natl Acad Sci U S A. 1993;90:292-296.
19. Perkin-Elmer Cetus Corporation. Rapid, efficient DNA extraction for PCR from cells or blood. Amplifications. 1989;2:1-3.
20. Moen CJA, van der Valk MA, Snoek M, et al. The recombinant congenic strains—a novel genetic tool applied to the study of colon tumor development in the mouse. Mamm Genome. 1991;1: 217-227.
21. Groot PC, Moen CJA, Dietrich W, Stoye JP, Lander ES, Demant P. The recombinant congenic strains for analysis of multigenetic traits: genetic composition. FASEB J. 1992;6:2826-2835.
22. Stassen APM, Groot PC, Eppig JT, Demant P. Genetic composition of the recombinant congenic strains. Mamm Genome. 1996;7:55-58.
23. Zarkowsky HS, Mohandas N, Speaker CB, Shohet SB. A congenital haemolytic anaemia with thermal sensitivity of the erythrocyte membrane. Br J Haematol. 1975;29:537-543.
24. Kuff EL, Lueders KK. The intracisternal A-particle gene family: structure and functional aspects. Adv Cancer Res. 1988;51:183-276.
25. Gwynn B, Lueders K, Sands MS, Birkenmeier EH. Intracisternal A-particle element transposition into the murine β-glucuronidase gene correlates with loss of enzyme activity: a new model for β-glucuronidase deficiency in the C3H mouse. Mol Cell Biol. 1998;18:6474-6481.
26. Ymer S, Tucker WQ, Campbell HD, Young IG. Nucleotide sequence of the intracisternal A-particle genome inserted 5′ to the interleukin-3 gene of the leukemia cell line WEHI-3B. Nucleic Acids Res. 1986;14:5901-5918.
27. Sonigo P, Wain-Hobson S, Bougueleret L, Tiollais P, Jacob F, Brulet P. Nucleotide sequence and evolution of ETn elements. Proc Natl Acad Sci U S A. 1987;84:3768-3771.
28. Shell BE, Collins JT, Elenich LA, Szurek PF, Dunnick WA. Two subfamilies of murine retrotransposon ETn sequences. Gene. 1990;86:269-274.
29. Shi Z-T, Afzal A, Coller B, et al. Protein 4.1R-deficient mice are viable but have erythroid membrane skeleton abnormalities. J Clin Invest. 1999; 103:331-340.
30. Wandersee NJ, Birkenmeier CS, Gifford EJ, Barker JE. Identification of three mutations in the murine erythroid alpha spectrin gene causing hereditary spherocytosis in mice [abstract]. Blood. 1998;92:8a.
31. Hassoun H, Coetzer TL, Vassiliadis JN, et al. A novel mobile element inserted in the α-spectrin gene: spectrin Dayton, a truncated α-spectrin associated with hereditary elliptocytosis. J Clin Invest. 1994;94:643-648.
32. Gallagher PG, Roberts WE, Benoit L, Speicher DW, Marchesi SL, Forget BG. Poikilocytic hereditary elliptocytosis associated with spectrin Alexandria: an αI/50b kd variant that is caused by a single amino acid deletion. Blood. 1993;82:2210-2215.
33. Fournier CM, Nicolas G, Gallagher PG, Dhermy D, Grandchamp B, Lecomte M-C. Spectrin St Claude, a splicing mutation of the human α-spectrin gene associated with severe poikilocytic anemia. Blood. 1997;89:4584-4590.
34. Allosio N, Wilmotte R, Maréchal J, et al. A splice site mutation of α-spectrin gene causing skipping of exon 18 in hereditary elliptocytosis. Blood. 1993;81:2791-2798.
35. Dalla Venezia N, Allosio N, Forissier A, et al. Elliptopoikilocytosis associated with the α469 His (Pro mutation in spectrin Barcelona (αI/50-49b). Blood. 1993;82:1661-1665.
36. Speicher DW, DeSilva TM, Speicher KD, Ursitti JA, Hembach P, Weglarz L. Location of the human red cell spectrin tetramer binding site and detection of a related "closed" hairpin loop dimer using proteolytic footprinting. J Biol Chem. 1993; 268:4227-4235.
37. Kotula L, DeSilva TM, Speicher DW, Curtis PJ. Functional characterization of recombinant human red cell α-spectrin polypeptides containing the tetramer binding site. J Biol Chem. 1993;268: 14788-14793.
38. Hassoun H, Wang Y, Vassiliadis J, et al. Targeted inactivation of murine band 3 (AE1) gene produces a hypercoagulable state causing widespread thrombosis in vivo. Blood. 1998;92:1785-1792.
39. Ohene-Frempong K, Weiner SJ, Sleeper LA, et al. Cerebrovascular accidents in sickle cell disease: rates and risk factors. Blood. 1998;91: 288-294.
40. Borgna-Pignatti C, Carnelli V, Caruso V, et al. Thromboembolic events in beta thalassemia major: an Italian multicenter study. Acta Haematol. 1998;99:76-79.
41. Holz A, Woldenberg R, Miller D, Kalina P, Black K, Lane E. Moyamoya disease in a patient with hereditary spherocytosis. Pediatr Radiol. 1998; 28:95-97.
42. Hayag-Barin JE, Smith RE, Tucker FC Jr. Hereditary spherocytosis, thrombosis, and chronic pulmonary emboli: a case report and review of the literature. Am J Hematol. 1998;57:82-84.
43. Nikol S, Huehns TY, Rainer R, Höfling B. Excessive arterial thrombus in spherocytosis: a case report. Angiology. 1997;48:743-748.